Mon. Not. R. Astron. Soc. **316**, 165–172 (2000)

Seismic study of stellar convective regions: the base of the convective envelope in low-mass stars

Mário J. P. F. G. Monteiro,[1,2] Jørgen Christensen-Dalsgaard[3] and Michael J. Thompson[4]
[1]*Centro de Astrofísica da Universidade do Porto, Rua das Estrelas, P-4150-762 Porto, Portugal*
[2]*Departamento de Matemática Aplicada da Faculdade de Ciências, Universidade do Porto, Portugal*
[3]*Teoretisk Astrofysik Center, Danmarks Grundforskningsfond, and Institut for Fysik og Astronomi, Aarhus Universitet DK-8000 Aarhus C, Denmark*
[4]*Astronomy Unit, School of Mathematical Sciences, Queen Mary & Westfield College, Mile End Road, London E1 4NS*

Accepted 2000 February 18. Received 2000 February 14; in original form 1999 November 9

ABSTRACT

The possibility of observing solar-type oscillations on other stars is of great relevance to investigating the uncertain aspects of the internal structure of stars. One of these aspects is the convective overshoot that takes place at the borders of the envelopes of stars of mass similar to, or lower than, the Sun. It affects the temperature stratification, mixing, rotation and magnetic-field generation. Asteroseismology can provide an observational test for the studies of the structure of such overshoot regions.

The seismic study of the transition in the Sun, located at the base of the convection zone, has been successful in determining the characteristics of this layer in the Sun. In this work we consider the extension of the analysis to other solar-type stars (of mass between 0.85 and $1.2\,M_{\odot}$) in order to establish a method for determining the characteristics of their convective envelopes. In particular, we hope to be able to establish seismologically that a star does indeed possess a convective envelope, to measure the size of the convective region and also to constrain the properties of an overshoot layer at the bottom of the envelope. The limitations in terms of observational uncertainties and stellar characteristics, and the detectability of an overshoot layer, are discussed.

Key words: convection – stars: evolution – stars: interiors – stars: oscillations.

1 INTRODUCTION

Convection and overshoot constitute a long-standing problem in stellar structure and evolution calculations. The difficulty in making progress has in part been because of the lack of observational constraints that can test directly the proposed formulations for modelling convection and its effects on the structure of a star. Convective overshoot, corresponding to a extension of convection into the stable regions, is known to occur at the borders of the convective envelope in the Sun, and is expected to be present also in other stars with convective regions. As for the Sun, asteroseismology may provide the tool necessary to study in some detail how convective overshoot affects the structure of such transition layers in stars.

Determining global properties of stellar convective envelopes would test theories of convection more comprehensively than a single solar determination. In the context of mixing-length theory, for instance, the Sun provides very precise constraints on the value of the mixing-length parameter; but that particular value may have no relevance for modelling other stars. Moreover, information from other stars is important for testing new formulations for stellar convection, and provides an essential complement to numerical simulations.

1.1 Overshoot and the modelling of stellar structure and evolution

There is little doubt that convective overshoot, to some extent, occurs at the borders of convective regions in stars; in the solar case, this has been indicated by numerical simulations of convection. Overshoot beyond the stability boundary is also clearly seen at the surface of the Sun. Similarly, convective overshoot is likely from convective cores in main-sequence stars more massive than the Sun. Significant effects on stellar evolution may result from overshoot both from convective cores (e.g. Maeder 1976; Herwig et al. 1997) and from convective envelopes (e.g. Alongi et al. 1991). Yet in most calculations of stellar evolution, overshoot is neglected. One of the reasons is the lack of a theory of convection which might predict the extent of the overshoot layer, as a function of stellar properties (for bounds on the extent, see Roxburgh 1992). Physical models for the overshoot (e.g. Shaviv & Salpeter 1973; Cogan 1975; Zahn 1991; Umezu 1995; Canuto 1997) provide estimates of the overshoot distance but themselves generally contain parameters which cannot be constrained from first principles; also, the inclusion of such formulations in stellar evolution codes is still complicated. A simpler procedure, which has been used in several calculations, is

to parametrize the extent of overshoot; very often, in analogy with the mixing-length parameter, the extent is taken to be a multiple of the pressure scaleheight at the convection-zone boundary. Constraints on this parameter, in the case of convective cores, have been obtained from comparison of models of open clusters or binary stars with observations (e.g. Andersen, Nordström & Clausen 1990; Kozhurina-Platais et al. 1997; Nordström, Andersen & Andersen 1997; Schröder, Pols & Eggleton 1997). However, it is of obvious interest to obtain more direct observational evidence about the properties and extent of the overshoot region, as may be possible from studies of the frequency signal considered here.

1.2 Seismic study of overshoot

Seismic studies of the base of the solar convective envelope have constrained the properties at that transition region (e.g. Basu, Antia & Narasimha 1994; Monteiro, Christensen-Dalsgaard & Thompson 1994 – hereafter MCDT; Roxburgh & Vorontsov 1994; Christensen-Dalsgaard, Monteiro & Thompson 1995 – hereafter CDMT), which is of relevance to mixing, rotation and magnetic activity (e.g. Monteiro, Christensen-Dalsgaard & Thompson 1998b, and references therein). An important implication is that the overshoot layer is not nearly adiabatic stratified, as in simple models: there is growing evidence that the effect on the temperature stratification is small in spite of an extended penetration region (e.g. Singh, Roxburgh & Chan 1995).

The method used is to identify in the frequencies of oscillation a characteristic signature originating from the base of the convection zone. That signature, corresponding to a periodic signal as a function of the frequency, can be isolated in the observed values and used to constrain the structure of the transition layer at the base of the convective envelope. For more distant stars, and in contrast to the Sun, only modes of very low degree are expected to be observed. That restricts our seismic analysis to a small number of modes, and some degree-dependent information is lost. Even so, the major properties of the signal, namely its period and amplitude (see Section 3), can still be determined if the observations have sufficiently low errors. The typical signal is a frequency modulation of order 0.1 μHz, which places very stringent limits on the detectability of the signal.

The modes of oscillation are characterized by their radial order n, which approximately corresponds to the number of nodes of the oscillation in the radial direction, and their degree l, which characterizes the horizontal wavelength of the oscillation. The properties of the oscillations, including the angular frequency ω_{nl}, reflect the resonance cavity that supports each oscillation mode. For acoustic modes, such as are relevant for solar-like oscillations, this dependence is given to leading order by the asymptotic expression (Tassoul 1980)

$$\omega_{nl} \sim \left(n + \tfrac{l}{2} + \tfrac{1}{4} + \alpha\right)\Delta\omega, \tag{1}$$

$\alpha(n,l)$ is owing to the change of phase occurring at the upper reflecting boundary, just beneath the surface, and

$$\frac{\Delta\omega}{2\pi} = \left(2\int_0^R \frac{\mathrm{d}r}{c}\right)^{-1} \equiv \frac{1}{2\tau_\mathrm{t}}, \tag{2}$$

where c is the local adiabatic sound speed, r the radial distance to the centre, and R the photospheric radius of the star. The quantity τ_t gives the total acoustic size of the star (the time an acoustic wave takes to go from the surface to the centre of the star). Observation of oscillation frequencies in a star allows us to determine $\Delta\omega$, which depends on the stellar mass and radius according to $\Delta\omega \propto \sqrt{M/R^3}$. Given that the determination of mass and radius is extremely difficult, in general, the determination of $\Delta\omega$ would be an important constraint on the global properties of a star.

However, the deviations from this asymptotic description of the frequencies contain important information about the internal structure of the star. That occurs, for example, when the stratification of a star varies rather abruptly, as at the edge of a convective region. It is this aspect that we address by determining the extent to which we can use the finer details in the frequency spectrum to measure the properties of convective envelopes in stars of mass similar to the solar value. Following the work of CDMT we first establish the expression for the signal in the frequencies owing to the transition region associated with the base of a convective envelope in these stars. Several models of different mass are then considered, some of these including overshoot, in order to determine the expected properties of the signal. We also address the changes of the signal with age. The detectability of the signal is discussed, in the light of the forthcoming programs for observing solar-like oscillations on other stars.

2 THE BASE OF A CONVECTIVE ENVELOPE

2.1 The derivative of the local sound speed

The adiabatic sound speed c plays a crucial role in determining the frequencies of the global p modes of a star. At the edge of a convective region the change in the temperature gradient from being radiative to the adiabatic value causes a discontinuity in the second derivative of the sound speed. This is illustrated in Fig. 1, which shows the run of the sound-speed derivative with acoustic depth for a zero-age solar model.

The adiabatic sound speed, which is an indirect measure of the temperature T, is given by $c^2 = \Gamma_1 p/\rho \propto T$, where p is pressure, ρ is density and adiabatic exponent $\Gamma_1 \equiv (\partial \log p/\partial \log \rho)_s$. This is why we can write the sound-speed derivative, with respect to

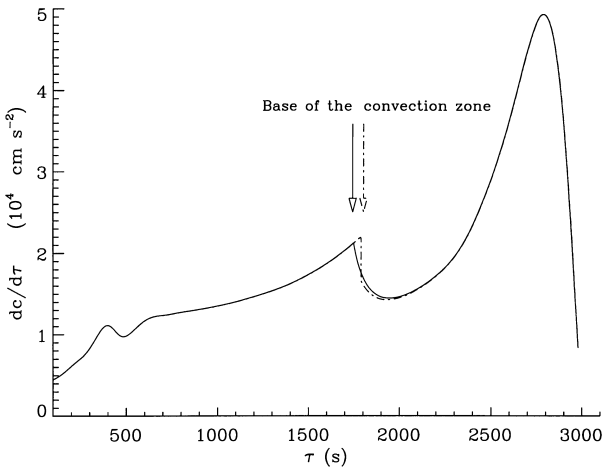

Figure 1. Derivative of the sound speed versus acoustic depth τ illustrating the sharp feature at the base of the convective envelope in zero-age main-sequence stars of a solar mass. One model does not incorporate overshoot of any form (continuous line) while the other has an adiabatically stratified overshoot layer of size $\ell_\mathrm{ov} = 0.189 H_\mathrm{p}$ (dashed–dotted line). Note also the small but relatively sharp bump at $\tau \simeq 400$ s which arises from the second ionization of helium and the associated variation in Γ_1, as well as the strong variation in the core.

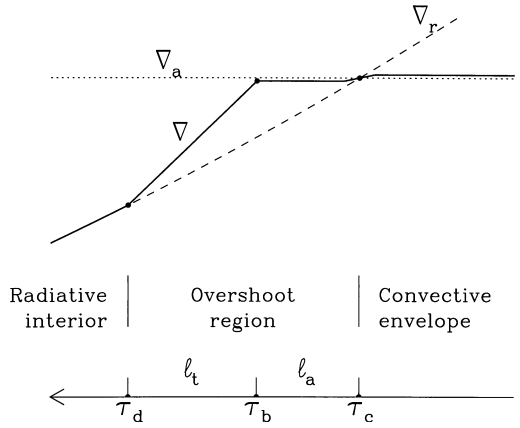

Figure 2. Sketch of the base of the convection zone showing the behaviour of the temperature gradient below the point τ_c where the superadiabatic gradient goes to zero (Schwarzschild boundary), down to τ_d where the velocity field goes also to zero (full radiative equilibrium is attained). Between τ_d and τ_c there is τ_b corresponding to the point separating the regions of efficient convection ($\tau_c \leqslant \tau \leqslant \tau_b$) and inefficient convection ($\tau_b \leqslant \tau \leqslant \tau_d$).

acoustic depth τ (the sound travel time measured from the photosphere; $\tau \equiv \int_r^R \mathrm{d}r/c$) in terms of the logarithmic temperature gradient $\nabla \equiv \mathrm{d}\log T/\mathrm{d}\log p$.

As shown by CDMT, near the base of the convective envelope for a solar-type star, we have that

$$\frac{\mathrm{d}c^2}{\mathrm{d}\tau} = d_{10} + d_{11}\frac{\nabla - \nabla_a}{\nabla_a}, \tag{3}$$

where (see Monteiro 1996, for further details)

$$d_{10} \equiv gc(\Gamma_1 - 1) \qquad \text{and} \qquad d_{11} \equiv gc(\gamma - 1). \tag{4}$$

Here, g is the gravitational acceleration, γ the ratio of the specific heats, while ∇_r and ∇_a are the radiative and adiabatic gradients, respectively.

The behaviour of $\mathrm{d}c/\mathrm{d}\tau$ in models with and without overshoot is illustrated in Fig. 1. The only term in equation (3) that contributes to the derivative in the convection zone is d_{10}. The change in the radiative interior occurs because ∇ becomes ∇_r, introducing the contribution from d_{11}. This is the origin of the discontinuity in the second derivative of the sound speed in the standard method of modelling the base of the convection zone.

The gradient at the base of the convection zone of a solar-type star can be expressed, approximately, according to (see Fig. 2)

$$\nabla - \nabla_a = (\nabla_r - \nabla_a) \times f(\tau), \tag{5}$$

where

$$f(\tau) \equiv \begin{cases} 0^+ & : \tau < \tau_c \quad \text{convection zone,} \\ 0 & : \tau = \tau_c \quad \text{Schwarzschild point,} \\ 0^+ & : \tau_c < \tau < \tau_b \quad \text{overshooting } (\ell_a), \\ f_t(\tau) & : \tau_b < \tau < \tau_d \quad \text{overshooting } (\ell_t), \\ 1 & : \tau \geqslant \tau_d \quad \text{radiative interior.} \end{cases} \tag{6}$$

The value of 0^+, in both the convection zone and the overshoot region, reflects the fact that the value of ∇ near the base, but inside the convection zone, is slightly superadiabatic, while in the overshoot region ($\tau_c < \tau < \tau_b$) the stratification is slightly subadiabatic. If there is no overshoot layer then we have $\tau_d = \tau_b = \tau_c$.

The unknown function $f_t(\tau)$ describes how the transition to a radiative stratification occurs, and so it establishes what fraction of the flux in each point of this region (of size ℓ_t) is transported by radiation.

From numerical simulations of convection (e.g. Singh et al. 1995) and from models of convective overshoot (e.g. Shaviv & Salpeter 1973; Canuto 1997), we do not expect just a simple transition from ∇_a in the envelope to ∇_r in the interior, with the jump taking place at the Schwarzschild boundary (where $\nabla_a = \nabla_r$). The shape of the transition, as given by the function $f_t(\tau)$, can change drastically the derivatives of the sound speed, affecting the response of the modes to this layer in the star.

2.2 Convective overshoot at the base of the envelope

A schematic description of the overshoot layer is presented in Fig. 2 where the two regions are shown: the region of near adiabatic stratification (of size ℓ_a), and the region where radiation takes over (of size ℓ_t). The region between τ_c and τ_b, of size ℓ_a, corresponds to the stable region where convective energy transport is still very efficient. Below the point τ_b we have a region of size ℓ_t where convection becomes less efficient, but where weak overshooting still takes place (so mixing and magnetic-field storage, for example, may occur). Numerical simulations of convection (Singh et al. 1995) and seismic studies of the overshoot layer indicate that the Sun may have a value of ℓ_t comparable to, if not larger than, ℓ_a.

We note that the method developed here is essentially only sensitive to ℓ_a. This aspect is pertinent when using seismic data to constrain models of overshoot. This is also the reason why we use here a simple, but extreme, model of overshoot for that region where the adiabatic stratification is extended into the convectively stable region, with an eventual discontinuous jump of size $\mathcal{D} \equiv (\nabla_r - \nabla_a)_{r_d}$ in the temperature gradient to its radiative value. This produces a discontinuity in the *first* derivative of the sound speed (and is equivalent to setting $\ell_t = 0$). Note that now we have a derivative of a discontinuous function (equation 3). This causes a larger, stronger signal since the frequencies are now perturbed by a much sharper transition at the base of the envelope.

3 THE SIGNAL IN THE FREQUENCIES

3.1 Expression for the signal

In order to describe how the frequencies are affected by the transition layer located at the base of a convective envelope we consider a variational principle for the mode frequencies. In this way it is possible to estimate the changes to the frequencies, as a perturbation $\delta\omega$ added to the reference value ω_0 of a fictitious star that has the sharp feature smoothed out. We have previously shown (MCDT; CDMT) how the edge of the convective region induces a contribution to this change that is a periodic function of the mode frequencies, regardless of whether there is convective overshoot or not; this periodic signal can be used to infer the properties of the boundary of the convection zone.

In stars other than the Sun only very low-degree modes are expected to be observed, and hence we can neglect the dependence on degree in the vicinity of the convective boundary. In that case the displacement eigenfunction describing the amplitude of the oscillation can be approximately written as

$$\xi_r \propto \frac{1}{r\sqrt{\rho c}}\cos[\omega(\tau + a_\phi) + \phi_0], \tag{7}$$

where $a_\phi \equiv -\pi\, \mathrm{d}\alpha/\mathrm{d}\omega$ ($\sim$200 s – see CDMT) and ϕ_0 are constants. The sensitivity of each mode to a particular region of the interior is proportional to the squared amplitude of the eigenfunction at that location. This is the origin of the periodic component of the change in the frequencies for low-degree modes owing to the transition region occurring at the base of a convective envelope (located at an acoustic depth of τ_d). It has the form (Monteiro 1996)

$$\delta\omega_p = \left(\frac{A_1^2}{\omega^4} + \frac{A_2^2}{\omega^2}\right)^{1/2} \cos[2(\omega\bar{\tau}_\mathrm{d} + \phi_0)]. \tag{8}$$

Here A_1 and A_2 are amplitudes that depend weakly on frequency ω: A_1 is always present in general, but A_2 will be non-zero only if there is overshoot, of the nature discussed above. Also, $\bar{\tau}_\mathrm{d} \equiv \tau_\mathrm{d} + a_\phi$ depends on acoustical depth τ_d of the edge of the convection zone measured from the surface of the star.

The signal is illustrated in Fig. 3, for four stellar models (with and without overshoot), using only modes with degrees $l = 0$, 1 and 2.

3.2 The expected amplitude of the signal

The value of the amplitude provides a measure of the type of transition at the base of the convective envelope of the star, including the properties of the stratification in the overshoot region. To facilitate the comparison between different stars, we consider the amplitude of the periodic signal evaluated at a fiducial frequency $\tilde{\omega}$ (see CDMT for details):

$$A_\mathrm{d} \equiv \left(\frac{A_1^2}{\tilde{\omega}^4} + \frac{A_2^2}{\tilde{\omega}^2}\right)^{1/2}$$

$$\simeq \frac{g(\gamma-1)}{8c\tilde{\omega}\tau_\mathrm{t}} \frac{1-\delta_\mathrm{c}}{\nabla_\mathrm{a}} \left[\left(\frac{1}{2\tilde{\omega}}\frac{\mathrm{d}\nabla_\mathrm{r}}{\mathrm{d}\tau}\right)^2 + (\nabla_\mathrm{r} - \nabla_\mathrm{a})^2\right]^{1/2}. \tag{9}$$

Here all quantities, including the correction term δ_c, are evaluated at the transition.

For the present-age Sun, we choose $\tilde{\omega}/2\pi = 2500\,\mu$Hz since this frequency is in the range where the signal from the base of the convection zone is clearest. We take this value and scale it for other stars (using standard homology scaling for frequencies): equation (9) gives an estimate of the dependence of the amplitude A_d on the properties of the transition. These estimates of the signal, which are computed from a stellar model, can be compared with the actual properties of the signal as determined from the global frequencies of the model.

The amplitude of the signal reflects the possible presence of

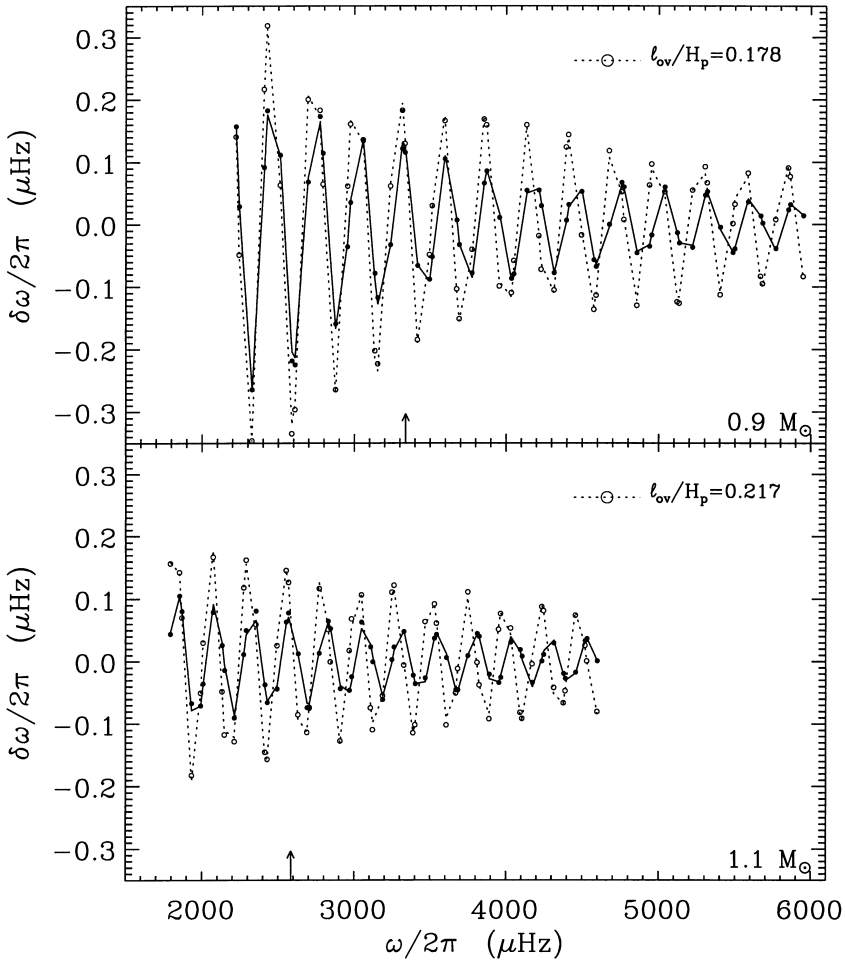

Figure 3. Signals from the edge of a convective envelope as detected in the frequencies from 0.9- (upper panel) and 1.1-$M_\odot$ (lower panel) zero-age main-sequence stellar models. The lines represent the fitted expression (equation 8) in the case of models incorporating overshoot (dotted line) and without overshoot (continuous line). The actual points to be fitted are shown as open and filled circles for both types of models. The arrows indicate the values of $\tilde{\omega}$ for the models.

convective overshoot, through the contribution from A_2, but is expected to change also because of changes in the internal structure of the star as it evolves.

3.3 Measuring the signal in the frequencies

From the p-mode frequencies of stellar models we can determine the amplitude and the period of the signal. We do so by fitting to the frequencies the expression for the signal (equation 8), obtaining the best values using a least-squares method for the parameters

$$A_1, \quad A_2, \quad \bar{\tau}_\mathrm{d} \quad \text{and} \quad \phi_0.$$

The fitting procedure used is a simplified version of the method described by MCDT, without the degree-dependent terms. This method uses an iterative process in order to remove the slowly varying trend of the frequencies, leaving the required signature given in equation (8). A polynomial in n is fitted to the frequencies of all modes of given degree l separately, using a regularized least-squares fit (viz Tikhonov regularization; e.g. Tikhonov 1963) with third-derivative smoothing. The residuals to those fits are then fitted for all degrees simultaneously with an expression of the form given by equation (8). The latter fit is the 'signal' from the base of the convection zone. This procedure is then iterated: at each iteration we remove from the frequencies the previously fitted signal and recalculate the smooth component of the frequencies. The iteration converges when there are no changes to the smooth component or the signal.

4 STELLAR MODELS

In order to find the limits for the amplitude of the signal for models with different mass and amount of overshoot, we have computed several stellar models. The computations were essentially as described by Christensen-Dalsgaard (1982), although with somewhat updated physics. In the evolution calculations, element diffusion and settling were ignored. As discussed in Section 2.2, we represent overshoot through a simplified description of the temperature gradient, assumed to be extended nearly adiabatically beyond the limit of convective instability, followed by an almost discontinuous jump to the radiative gradient. Referring to expressions (5) and (6), in our stellar models the simplified formulation for overshoot assumes that $\tau_\mathrm{b} \equiv \tau_\mathrm{d}$. The extent of overshoot is parametrized by the size $\mathcal{D}$ of the discontinuity in ∇, defining the depth τ_d of the edge of the overshoot region such that $\nabla_\mathrm{a} - \nabla_\mathrm{r} = \mathcal{D}$ at τ_d; in the overshoot region it is assumed that $\nabla = \nabla_\mathrm{a}$.

We first consider several models on the zero-age main sequence (ZAMS), with masses between 0.85 and 1.2 solar masses, both without and with overshoot (the values for some of these are included in Table 1). For each value of the mass we have calculated six models with $\mathcal{D}$ between 0.0 (no overshoot) and 0.125 ($\ell_\mathrm{ov} > 0.2 H_\mathrm{p}$). It might be noticed that the convective envelope occupies a larger acoustic fraction of the star for lower mass stars. Near our upper mass limit, the models show a small convective core. As long as the core has a small acoustic size, the signal originating from its border does not affect the analysis discussed here (cf. Monteiro et al. 1998a; for more on the effect of convective cores, see, e.g., Audard, Provost & Christensen-Dalsgaard 1995).

From the expressions for the amplitude (equation 9) we can determine the expected values; these are given in Table 2. Several models of an evolved Sun, for different amounts of overshoot, have also been calculated in order to estimate how the properties of the signal in the frequencies change with evolution on the main sequence. The evolved models are listed in Table 3, together with their zero-age counterparts.

Table 1. Characteristics of some of the ZAMS models considered in this work with mass from 0.85 up to 1.2 $\mathrm{M}_\odot$. The total acoustic radius τ_t and the acoustic depth τ_d of the transition in the temperature gradient are in seconds. The overshoot layer has been modelled as being (essentially) adiabatically stratified and having a size ℓ_ov, here given in units of the local pressure scaleheight H_p. Also, $\mathcal{D}$ is the assumed discontinuity in ∇ at the edge of the overshoot layer.

$M/\mathrm{M}_\odot$	τ_t	τ_d	r_d/R	$\ell_\mathrm{ov}/H_\mathrm{p}$	$\mathcal{D}$
0.9	2648.8	1616.4	0.6988	0.0000	0.000
0.9	2649.1	1632.7	0.6917	0.0824	0.050
0.9	2649.9	1652.1	0.6832	0.1784	0.100
0.9	2651.3	1663.8	0.6782	0.2335	0.125
1.0	2980.7	1749.0	0.7242	0.0000	0.000
1.0	2981.0	1768.1	0.7172	0.0869	0.050
1.0	2981.7	1790.8	0.7088	0.1886	0.100
1.0	2983.3	1804.4	0.7040	0.2455	0.125
1.1	3414.1	1862.6	0.7638	0.0000	0.000
1.1	3414.5	1887.5	0.7566	0.1004	0.050
1.1	3415.8	1917.0	0.7480	0.2166	0.100
1.1	3417.0	1934.2	0.7430	0.2826	0.125
1.2	3931.7	1838.4	0.8266	0.0000	0.000
1.2	3932.0	1867.2	0.8206	0.1064	0.050
1.2	3933.1	1902.1	0.8133	0.2333	0.100
1.2	3934.2	1922.1	0.8091	0.3042	0.125

Table 2. Results obtained by interpolating values found from the fit of the signal in the frequencies for all models considered (some are listed in Table 1). Acoustic depths (τ_d and $\bar{\tau}_\mathrm{d}$) are in seconds, and the amplitude A_d is in μHz.

$M/\mathrm{M}_\odot$	$\ell_\mathrm{ov}/H_\mathrm{p}$	τ_d (expected)	$A_\mathrm{d}/2\pi$	$\bar{\tau}_\mathrm{d}$ (fitted)	$A_\mathrm{d}/2\pi$
0.9	0.0	1616.4	0.143	1747.2	0.131
1.0	0.0	1749.0	0.125	1884.1	0.098
1.1	0.0	1862.6	0.098	2036.0	0.072
1.2	0.0	1838.4	0.090	2028.3	0.059
0.9	0.1	1636.4	0.146	1757.0	0.166
1.0	0.1	1771.0	0.125	1898.4	0.127
1.1	0.1	1887.4	0.100	2044.8	0.094
1.2	0.1	1865.5	0.087	2034.8	0.076
0.9	0.2	1656.7	0.206	1777.8	0.229
1.0	0.2	1793.4	0.181	1925.4	0.186
1.1	0.2	1912.7	0.144	2070.3	0.140
1.2	0.2	1893.0	0.128	2061.7	0.116

5 MEASURED PROPERTIES FROM THE SIGNAL IN THE FREQUENCIES

For all models considered (e.g. Table 1) we have calculated the frequencies for their linear adiabatic oscillations corresponding to acoustic modes of oscillation. Only very low-degree modes ($l \leqslant 2$) have been considered, in a range of frequencies

Table 3. Results found from the fit of the signal in the frequencies for models of a solar mass but different ages. Acoustic depths (τ_d and $\bar{\tau}_d$) are in seconds, and the amplitude A_d is in μHz.

Age (10^9 yr)	ℓ_{ov}/H_p	τ_d (expected)	$A_d/2\pi$	$\bar{\tau}_d$ (fitted)	$A_d/2\pi$
0.00	0.000	1749.0	0.125	1884.1	0.098
0.00	0.042	1758.1	0.116	1887.0	0.104
0.00	0.087	1768.1	0.120	1895.3	0.120
0.00	0.136	1779.1	0.142	1907.9	0.146
0.00	0.189	1790.8	0.174	1922.3	0.179
0.00	0.246	1804.4	0.209	1938.2	0.215
4.53	0.000	2065.7	0.072	2236.3	0.061
4.53	0.045	2077.3	0.070	2239.0	0.066
4.53	0.094	2089.9	0.079	2249.0	0.081
4.53	0.146	2103.6	0.100	2263.8	0.102
4.53	0.203	2118.8	0.124	2280.7	0.125
4.53	0.264	2135.4	0.152	2301.1	0.150

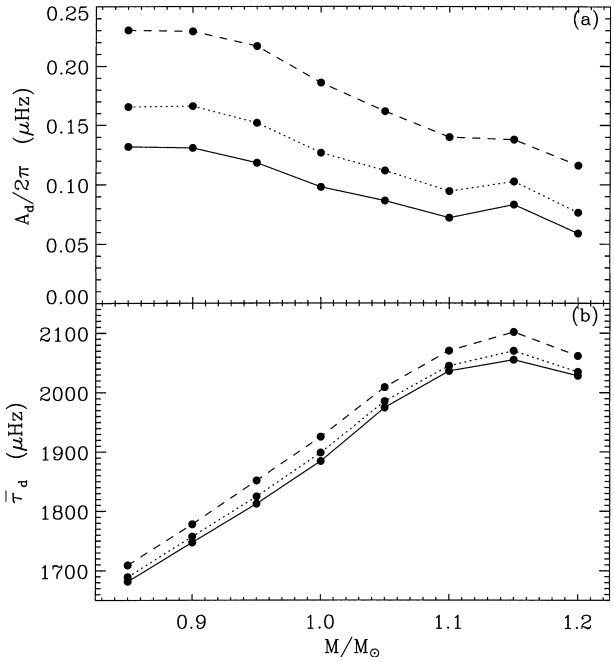

Figure 4. Results given in Table 2, as found from interpolating the values of the parameters from the fit of equation (8) to the frequencies of the computed ZAMS models. The dashed line joins values for models with an overshoot layer of size $\ell_{ov} = 0.2H_p$, while the dotted line is for models with $\ell_{ov} = 0.1H_p$ and the continuous line for $\ell_{ov} = 0.0H_p$.

corresponding approximately to the modes observed in the Sun (suitably scaled according to $\sqrt{M/R^3}$). We then use these frequencies to fit the expression of the signal as described in Section 3.3. For each model we have obtained the set of four parameters which we can use here to establish the dependence of the signal on the properties of each star at the base of the convective envelope. Examples of the 'signals' isolated in the frequencies of oscillations are shown in Fig. 3.

The acoustic depth $\bar{\tau}_d$ is the parameter most easily measured in the frequencies because it simply gives the period of the signal. However, owing to the contribution from a_ϕ (see equation 7), it does not provide a direct measurement of the acoustic size τ_d of the envelope. This can be seen in Table 2, where the systematic difference between τ_d and $\bar{\tau}_d$ is just an indication of the value of a_ϕ for the models considered.

The amplitude of signal is a function of frequency (equation 8), requiring care in the fits in order to isolate this signal from other contributions also present in the frequencies. The physical interpretation of the amplitude is provided by equation (9). In particular, the presence of overshoot as reflected in A_2, with the present sharp transition as determined by the value of $\mathcal{D}$, leads to an increased amplitude which is consequently easier to fit (see also Fig. 4a). We note, however, that the behaviour would be different if the assumption of having an adiabatically stratified overshoot layer followed by a sharp transition were relaxed (cf. CDMT). Therefore the results found for the overshoot models presented here must be taken as an upper limit for the amplitude of the signal.

Before proceeding, it is worth commenting why in what follows we generally discuss only A_d and not the individual contributions from A_1 and A_2. For small observational errors, the recovered A_1 and A_2 are able to reproduce the expected behaviour (MCDT; Monteiro 1996). Their individual values can be used to constrain the properties of the overshoot as indicated by equation (9). However, in the presence of large observational errors the frequency dependence is blurred (MCDT), coupling the two coefficients. Thus we instead consider A_d in our discussion of the properties of the observed signal, since its value is much less affected by the observational errors.

5.1 Dependence on stellar mass

To illustrate in more detail the dependence of the signal on stellar mass and overshoot, Table 2 lists the results obtained by fitting the frequencies of the ZAMS models. The amplitudes and acoustic depths from the fits are shown in Fig. 4. There is a clear increase of the measured amplitude for decreasing stellar mass.

We also find an increase of the measured acoustic depth with stellar mass which reflects the increase in total acoustic depth of the star (see Table 1) although the radial size of the envelope decreases for the more massive stars.

5.2 Effect of convective overshoot on the amplitude

The amplitude of the signal inferred from the frequencies is smallest for models that have no convective overshoot. Any extension of the convection zone by overshooting, of the type considered here, will give a larger amplitude: the actual value depends on the type of stratification imposed and the extent of the overshoot layer. In our simple analysis this is reproduced quantitatively by the term A_2 (equation 9), which increases with the increase in the jump of the logarithmic temperature gradient as specified by $\mathcal{D}$. It is evident that, for each mass, models with overshoot have a substantially larger amplitude. Thus we may hope to be able to discriminate between these cases if the mass of the star is known with sufficient accuracy.

Table 2 also lists amplitudes expected from the analytical expressions (equation 9). In models with substantial overshoot, with $\ell_{ov} > 0.1H_p$, say, these are in reasonable agreement with the values obtained for the fit. In models with little or no overshoot, on the other hand, there are substantial discrepancies; in particular, the expected amplitude initially decreases in the 1.2-M$_\odot$ model, when overshoot is introduced. A similar behaviour is shown in Fig. 5. This was also found by CDMT in the solar case, as well as

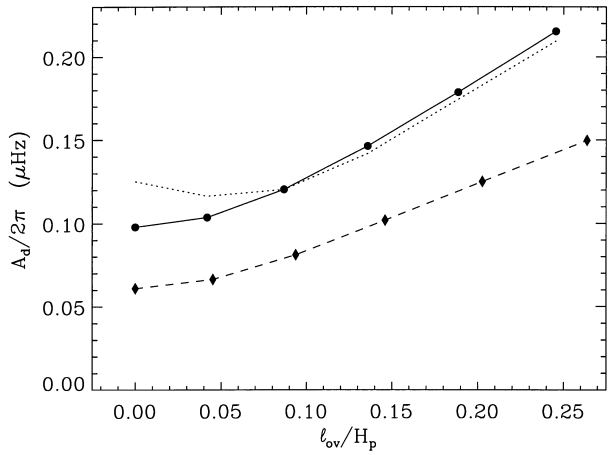

Figure 5. Expected amplitudes for the signal in the frequencies (dotted line) and the values found by fitting the signal in the frequencies (filled circles). The values shown are for zero-age (filled circles–continuous line) and evolved (filled diamonds–dashed line) stellar models of 1 solar mass having different overshoot layers at the bottom of the convective envelope (Table 3). These illustrate the change owing to evolution from the zero age up to an age of 4.53×10^9 yr.

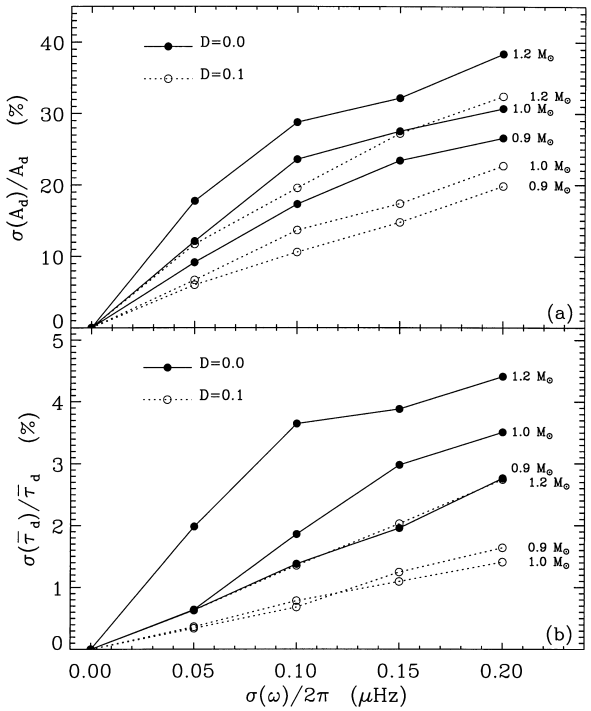

Figure 6. Relative errors in percentage for the amplitude A_d (panel a) and acoustic size of the envelope $\bar{\tau}_d$ (panel b), as found from the fit of the frequencies for different values of the observational errors $\sigma(\omega)$, assuming that approximately 60 frequencies of modes with $l = 0$–2 have been measured. The dotted lines are for models with overshoot (as modelled by setting $\mathcal{D} = 0.1$) while the continuous lines are for models with no overshoot. The value of the mass (in units of a solar mass $M_\odot$) is indicated for each set of points connected by a line.

by Roxburgh & Vorontsov (1994) who put some emphasis on this behaviour. However, we stress that the fitted amplitudes show no such behaviour: overshooting increases the amplitude of the signal obtained by fitting the frequencies.

5.3 Changes with the aging of the star

To investigate the dependence on age, Table 3 shows results for a 1-$M_\odot$ model at close to solar age (see also Fig. 5). The amplitude decreases with age; this must also be taken into account when testing the models against the observations. In particular, for the Sun we have, from Table 3, that

$$\frac{A_{d,\odot}(\text{now})}{A_{d,\odot}(\text{ZAMS})} \simeq 0.59. \tag{10}$$

Thus the amplitude of the signal decreases by about 40 per cent over this time-span. Part of the change (about 15 per cent) is consistent with a simple homologous scaling for the frequency as the radius increases with age. The remaining part (about 25 per cent) arises because of changing conditions at the base of the convection zone, particularly the details of opacity, as the extent of the convection zone changes with age.

5.4 Detectability of the signal

In the present case, where only modes of very low degree are considered, the fitting is very sensitive to the number of modes used for each value of l. Because the smoothing procedure of our method uses the third derivative (see Section 3.3), it imposes a lower limit of four modes for each value of the degree. Also, as a result of the fact that we are quite likely restricted to $l \leqslant 2$, it is necessary to ensure that we have enough modes to resolve the oscillatory signal. Thus we need at least about six mode frequencies for each value of l, even with noise-free frequency data. The minimum number of modes needed to isolate the signal increases with increasing observational errors.

The ratio of the amplitude of the periodic signal to the fiducial frequency gives a feel for the accuracy with which we need the frequencies of the star to be determined. Estimating the value of the amplitude from stellar models (Table 1), we find that the signal in the frequencies is typically a few parts in 10^5.

The present observational uncertainties $\sigma(\omega)/\omega$ for the Sun are below 10^{-6}: the resulting estimated error for the determination of A_d is below 5 per cent. A similar precision for other stars of this order of magnitude may be difficult to obtain. Nevertheless we expect to measure their very low-degree modes with a precision of a few parts in 10^5.

In order to determine how the observational uncertainties affect the determination of A_d we have performed Monte-Carlo simulations of the errors for different observational uncertainties. In particular, we have calculated from 200 error realizations what is the error $\sigma(A_d)$ in the determination of A_d, and also the error $\sigma(\bar{\tau}_d)$ in the determination of $\bar{\tau}_d$, for observational errors $\sigma(\omega)/2\pi$ up to 0.20 μHz; approximately 60 modes (20 per degree l) were included in the analysis. The results are shown in Fig. 6, for different stellar masses and for cases without and with overshoot. It is evident that the stronger signal in the presence of overshoot reduces the sensitivity of the results to observational errors.

If fewer frequencies are available, the constraints on the errors are correspondingly stricter. None the less, if the observational uncertainties are below about 0.1 μHz, reasonable accuracy can be achieved. For example, we have conducted numerical experiments

with fewer modes from a 1.0-$M_\odot$ star with no overshoot, and with observational uncertainties of 0.1 μHz on the frequencies. With just 30 modes in total, the relative uncertainties on the inferred values of $\bar{\tau}_d$ and A_d are 4.3 and 27 per cent respectively; even with just 18 modes (but these restricted to mode orders $n \leqslant 20$), the corresponding uncertainties we obtain are only 5.1 and 44 per cent.

6 DISCUSSION

A method to determine the properties of the base of the convective envelope in low-mass stars ($0.85 \leqslant M/M_\odot \leqslant 1.2$) using the frequencies of very low-degree modes has been discussed. If enough modes (more than 10 for each l value) for degrees up to $l = 2$ are available then the signal in the frequencies can be measured if we have sufficiently accurate observations, with $\sigma(\omega)/2\pi \leqslant 0.1$ μHz. The detectability of the signal improves significantly if more modes are added, and in particular if we can add modes of degree $l = 3$.

We have demonstrated what information regarding the properties of convective overshoot can be obtained from such an analysis. This, together with the determination of the acoustic size of the envelope, can provide additional constraints to test theories of convection and overshoot. In particular, it is highly desirable to confirm the behaviour found for the Sun, namely that the stratification of the overshoot region is apparently nearly radiative, contrary to the initial predictions and current modelling of the effect of overshoot in stellar evolution.

We have also investigated how aging affects the properties of the signal, and found that this effect must be taken into account when constraining the properties of stellar models. In particular, for the Sun the amplitude of the signal decreased by about 40 per cent from the ZAMS to the present time. We note that the age of the star can be constrained from the observed value of the small frequency separation $\omega_{n\ l} - \omega_{n-1\ l+2}$ (e.g. Christensen-Dalsgaard 1984, 1988; Ulrich 1986).

Several space missions have been planned for observing solar-type oscillations in other stars: *COROT* (Baglin et al. 1998), *MOST* (Matthews 1998) and *MONS* (Kjeldsen & Bedding 1998). These are expected to provide data on a few stars with the accuracy required by our analysis. That allows us to hope that in the not too distant future we may have additional significant constraints for testing theories of convection and overshoot in stars.

ACKNOWLEDGMENTS

This work was supported in part the Danish National Research Foundation through its establishment of the Theoretical Astrophysics Center, by the Portuguese Fundação para a Ciência e a Tecnologia (grant PESO/P/PRO/1196/97), and by the UK Particle Physics and Astronomy Research Council.

REFERENCES

Alongi M., Bertelli G., Bressan A., Chiosi C., 1991, A&A, 244, 95
Andersen J., Nordström B., Clausen J. V., 1990, ApJ, 363, L33
Audard N., Provost J., Christensen-Dalsgaard J., 1995, A&A, 297, 427
Baglin A., COROT team, 1998, in Deubner F.-L., Christensen-Dalsgaard J., Kurtz D. W., eds, Proc. IAU Symp. 185, New eyes to see inside the Sun and stars. Kluwer, Dordrecht, p. 301
Basu S., Antia H. M., Narasimha D., 1994, MNRAS, 267, 209
Canuto V. M., 1997, ApJ, 489, L71
Christensen-Dalsgaard J., 1982, MNRAS, 199, 735
Christensen-Dalsgaard J., 1984, in Praderie F., ed., Space Research Prospects in Stellar Activity and Variability. Paris Observatory Press, Paris, p. 11
Christensen-Dalsgaard J., 1988, in Christensen-Dalsgaard J., Frandsen S., eds, Proc. IAU Symp. 123, Advances in helio- and asteroseismology. Reidel, Dordrecht, p. 295
Christensen-Dalsgaard J., Monteiro M.J.P.F.G., Thompson M. J., 1995, MNRAS, 276, 283 (CDMT)
Cogan B. C., 1975, ApJ, 201, 637
Herwig F., Blöcker T., Schönberner D., El Eid M., 1997, A&A, 324, L81
Kjeldsen H., Bedding T. R., 1998, in Kjeldsen H., Bedding T. R., eds, Proc. Workshop on Science with a Small Space Telescope. Aarhus University, Aarhus, p. 1
Kozhurina-Platais V., Demarque P., Platais I., Orosz J. A., Barnes S., 1997, AJ, 113, 1045
Maeder A., 1976, A&A, 47, 389
Matthews J. M., 1998, in Korzennik S. G., Wilson A., eds, Proc. SOHO6/GONG98 Workshop, Structure and dynamics of the interior of the Sun and Sun-like stars. ESA SP-418. ESA Publications Division, Noordwijk, the Netherlands, p. 395
Monteiro M. J. P. F. G., 1996, PhD thesis, Queen Mary & Westfield College, Univ. London
Monteiro M. J. P. F. G., Christensen-Dalsgaard J., Thompson M. J., 1994, A&A, 283, 247 (MCDT)
Monteiro M. J. P. F. G., Christensen-Dalsgaard J., Thompson M. J., 1998a, in Deubner F.-L., Christensen-Dalsgaard J., Kurtz D. W., eds, Proc. IAU Symp. 185, New eyes to see inside the Sun and stars. Kluwer, Dordrecht, p. 315
Monteiro M. J. P. F. G., Christensen-Dalsgaard J., Thompson M. J., 1998b, in Korzennik S. G., Wilson A., eds, Proc. SOHO6/GONG98 Workshop, Structure and dynamics of the interior of the Sun and Sun-like stars. ESA SP-418. ESA Publications Division, Noordwijk, the Netherlands, p. 495
Nordström B., Andersen J., Andersen M. I., 1997, A&A, 322, 460
Roxburgh I. W., 1992, A&A, 266, 291
Roxburgh I. W., Vorontsov S. V., 1994, MNRAS, 268, 880
Schröder K.-P., Pols O. R., Eggleton P. P., 1997, MNRAS, 285, 696
Shaviv G., Salpeter E. E., 1973, ApJ, 184, 191
Singh H. P., Roxburgh I. W., Chan K. L., 1995, A&A, 295, 703
Tassoul M., 1980, ApJS, 43, 469
Tikhonov A. N., 1963, Sov. Maths.-Dokl., 4, 1035
Ulrich R. K., 1986, ApJ, 306, L37
Umezu M., 1995, MNRAS, 276, 1287
Zahn J.-P., 1991, A&A, 252, 179

This paper has been typeset from a TEX/LATEX file prepared by the author.